

Improved Offset-QAM OFDM Scheme with Enhanced Dispersion Tolerance

Jian Zhao¹ and Lian-Kuan Chen²

¹Phonic Systems Group, Tyndall National Institute and University College Cork, Lee Maltings, Dyke Parade, Cork, Ireland

²Department of Information Engineering, the Chinese University of Hong Kong, Shatin, N.T., Hong Kong
jian.zhao@tyndall.ie

Abstract: We propose a novel offset-QAM OFDM scheme to improve the dispersion tolerance to that of one subcarrier without cyclic prefix. This scheme exhibits greatly enhanced spectral efficiency compared to CP-OFDM and lower complexity than RGI-OFDM.

OCIS codes: (060.2330) Fiber optics communications; (060.4080) Modulation.

1. Introduction

Offset quadrature amplitude modulation (QAM) OFDM has attracted much attention in optical communications [1-4]. Compared to conventional OFDM, this technology can greatly relax the length of cyclic prefix (CP) for dispersion compensation and achieve ~20% increase in net data rate for the same transmission reach. On the other hand, it reduces the memory length of pulse-shaping filters and results in lower complexity than Nyquist FDM.

In previous works, the dispersion tolerance of the conventional offset-QAM OFDM scheme was found to scale with $T^2 \cdot N / \pi^2$, where T and N are the time interval between samples and the number of subcarriers, respectively. In this paper, we propose a novel offset-QAM OFDM scheme, which can further enhance the dispersion tolerance by a factor of N . Simulation results show that the proposed scheme can support a 224-Gbit/s polarization-division-multiplexing (PDM) offset-QPSK OFDM signal over dispersion of ~160,000 ps/nm without any CP. We also show that this scheme exhibits advantages of improved spectral efficiency, larger dispersion tolerance, or reduced complexity compared to CP-OFDM and reduced-guard-interval (RGI) OFDM using frequency domain equalization.

2. Principles

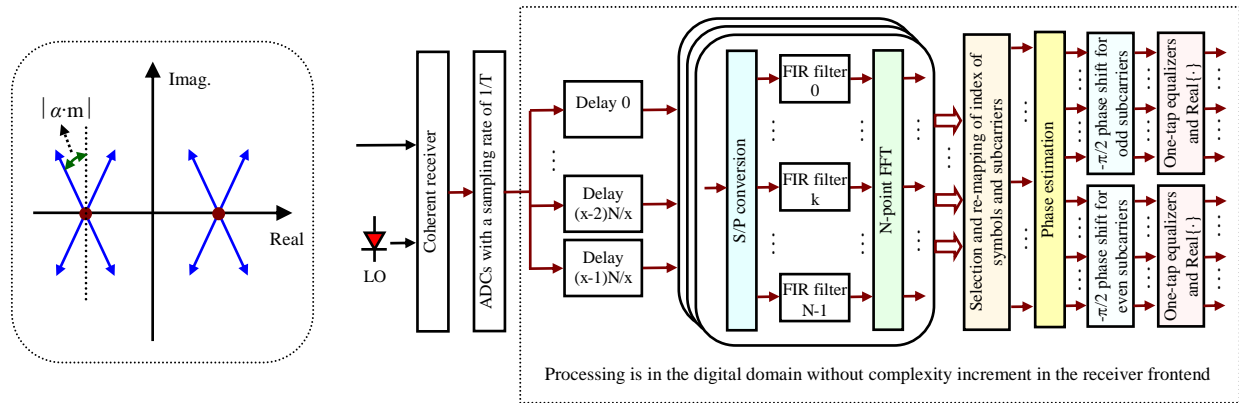


Fig. 1 Left: Relationship between the signal and the ICI in the conventional offset-QAM OFDM scheme. The in-phase tributary of a subcarrier in offset-4QAM OFDM is illustrated. Right: Setup of the proposed scheme.

In offset-QAM OFDM, the quadrature tributary of each subcarrier is delayed by half symbol period with respect to its in-phase tributary [2]. Without the loss of generality, the decoded in-phase tributary of the m^{th} subcarrier in the i^{th} OFDM symbol, $b_{i,m}^{\text{real}}$, in the conventional offset-QAM scheme can be derived as:

$$b_{i,m}^{\text{real}} = \exp(j\pi m/2 + j \cdot \alpha \cdot m^2) \cdot (A \cdot a_{i,m}^{\text{real}} + I_{i,m}^{\text{real}} + j \cdot c_{m,m}^{\text{imag}} + j \cdot \exp(j \cdot \alpha \cdot m) \cdot (c_{m+1}^{\text{real}} + c_{m+1}^{\text{imag}}) + j \cdot \exp(-j \cdot \alpha \cdot m) \cdot (c_{m-1}^{\text{real}} + c_{m-1}^{\text{imag}})) \quad (1)$$

where $a_{i,m}^{\text{real}}$ is the transmitted in-phase tributary of the m^{th} subcarrier data in the i^{th} OFDM symbol. A , $I_{i,m}^{\text{real}}$, $c_{m,m}^{\text{imag}}$, c_{m+1}^{real} , c_{m+1}^{imag} , c_{m-1}^{real} , c_{m-1}^{imag} are all real values, and represent the signal attenuation coefficient, inter-symbol interference (ISI), the crosstalk from the quadrature tributary of the m^{th} subcarrier and the in-phase and quadrature tributaries of the $(m+1)^{\text{th}}$ and $(m-1)^{\text{th}}$ subcarriers. $\alpha = \beta_2 \cdot L \cdot (2\pi / (TN))^2 / 2$ with $\beta_2 L$ being the accumulated dispersion. In practice, the term $\exp(j\pi m/2 + j \cdot \alpha \cdot m^2)$ can be compensated via channel equalization [3]. The key information provided by Eq. (1) is

that in addition to ISI, all crosstalk terms have a coefficient of either $\exp(j\cdot\alpha\cdot m)$ or $\exp(-j\cdot\alpha\cdot m)$. Fig. 1 (left) depicts the relationship between the signal and the ICI. When $|\alpha\cdot m| \ll 1$, $\exp(j\cdot\alpha\cdot m) \approx 1$. The desirable signal is real while all crosstalk terms are imaginary, so that the signal can be correctly decoded by extracting the real part after channel equalization. However, for a large value of dispersion, the crosstalk is no longer orthogonal to the signal. The dispersion tolerance is limited by the condition of $|\alpha\cdot m| < 1$ and scales with $T^2\cdot N/\pi^2$. Fig. 1 (right) shows the block diagram of the proposed scheme. The received signal is split into x paths, with the k^{th} path experiencing a time delay of kNT/x or a sample delay of kN/x in the digital domain. These delayed versions are then processed using FIR filters and the FFT individually, with each processing unit similar to that of the conventional offset-QAM OFDM scheme. When there is no dispersion, all subcarrier data in the i^{th} OFDM symbol, $a_{i,n}^{\text{real}}$, $-N/2+1 \leq n \leq N/2$, are decoded by the first processing unit (with zero delay) at the time $i\cdot N$. In the presence of a large value of dispersion, the pulse of a subcarrier (denoted as m) may delay into the time window of other processing units or even other OFDM symbol periods. $a_{i,m}^{\text{real}}$ in the i^{th} OFDM symbol should be decoded by the k^{th} processing unit at the time $(D+i)\cdot N$ if $(DNT + kNT/x)$ is the closest value to the relative delay of the m^{th} subcarrier. For example, for 4 paths (path 0–3) with sample delays of 0, $N/4$, $N/2$, and $3N/4$, when a subcarrier exhibits a delay of $1.1NT$, this subcarrier is decoded by path 0 and the decoded data at the time $i\cdot N$ in the digital domain corresponds to that in the $(i-1)^{\text{th}}$ OFDM symbol at the transmitter. When $(DNT + kNT/x)$ is ideally equal to the delay of the m^{th} subcarrier, we can analytically prove that the desirable signal and the crosstalk are orthogonal regardless of the dispersion:

$$b_{i,m}^{\text{real}} = \exp(j\pi m/2 - j\cdot\alpha\cdot m^2) \cdot (a_{i,m}^{\text{real}} + j\cdot c_{m+1}^{\text{real}} + j\cdot c_{m-1}^{\text{real}} + j\cdot c_m^{\text{imag}} + j\cdot c_{m+1}^{\text{imag}} + j\cdot c_{m-1}^{\text{imag}}) \quad (2)$$

When there is a timing misalignment between the pulse of a subcarrier and the optimal DFT window for this subcarrier, the performance degradation of the decoded signal on this subcarrier is similar to that analysed in Eq. (1). However, the maximum misalignment is half the delay interval between paths ($\propto 1/x$). For example, the maximum misalignment is $N/8$ and $N/16$ for x of 4 and 8, respectively. On the other hand, the complexity of demultiplexing (the FIR filters and FFTs in the boxes in Fig. 1) increases linearly with x so its value should be chosen to balance the performance and complexity. After parallel processing, the outputs of all processing units are sent into a decision unit, which re-maps the outputs of the processing units to the appropriate index of the decoded subcarriers and symbols. After the re-mapping unit, phase and channel are compensated and the signal is sent for data decoding.

3. Simulation results

We simulated 224-Gbit/s PDM offset-QPSK OFDM and CP-OFDM. The sampling rate of digital-to-analogue converters (DACs) was 80 GS/s. The number of subcarriers varied from 16 to 256. For each case, the number of zero-padded subcarriers in the high-frequency region was controlled such that the signal line rate (including the CP in CP-OFDM) was fixed to be 224 Gbit/s. In offset-QAM OFDM, the FIR filters created a square-root-raised-cosine function with a roll-off factor of 0.5. After DACs, low-pass filters with 40-GHz bandwidth were used to remove the aliasing. The signals of two polarizations were modulated, combined, and launched into fiber links. Nonlinearity in the fiber was not considered. At the receiver, the signals were filtered by an 80-GHz optical filter and coherently detected. The bandwidth of the receiver front end was 60 GHz and the sampling rate of analogue-to-digital converters was 80 GS/s. The number of simulated QPSK symbols was 200,000.

Fig. 2(a) shows the time index (normalized by N) to decode different subcarriers. In theory, this index is equal to $D + k/x$ as discussed above. It is seen that for a dispersion of 42,500 ps/nm, the subcarriers in one OFDM symbol may span over 12 OFDM symbols. In practice, the integer part of the delay of a subcarrier with respect to the time period of one OFDM symbol does not influence the performance, provided that the index of the transmitted and decoded symbols can be re-mapped correctly. In contrast, the number of paths determines the maximum timing misalignment between the pulse of a subcarrier and the optimal DFT window for this subcarrier. Fig. 2(b) shows the index of paths to decode different subcarriers (circles) and the remainder of normalized delays after taking the integer part (solid). The remainder of the normalized delay, in theory, is $(D_a - DNT)/(NT)$, where D_a is the actual delay of a subcarrier. It can be seen that the proposed algorithm indeed selects the path k with $(DNT + kNT/x)$ being the closest value to the actual delay of a subcarrier D_a , and the maximum misalignment is half of the delay interval between paths. Fig. 2(c) depicts the required OSNR versus dispersion. It can be seen that conventional offset-QAM OFDM can improve the dispersion tolerance by a factor of ~ 3 compared to CP-OFDM with zero CP. The proposed algorithm can further improve the tolerance by $\sim N$ times, from 1,300 ps/nm to 160,000 ps/nm at 20-dB OSNR.

Fig. 3(a) shows the dispersion tolerance versus the number of subcarriers. Conventional offset-QAM OFDM exhibits a similar tolerance as that of CP-OFDM with 18.75% CP and these tolerances scale linearly with the number of subcarriers. However, even when 1024 subcarriers are used, the tolerance of the conventional systems is

still limited below $\sim 1,000$ km. In contrast, the proposed scheme exhibits greatly enhanced tolerance even compared to CP-OFDM with 100% CP and this advantage increases as the number of subcarriers grows because the dispersion tolerance scales with the square of the number of subcarriers. The elimination of additional CP would result in significant enhancement in the net spectral efficiency. Fig. 3(b) shows the normalized spectral efficiency of CP-OFDM and the proposed scheme. It can be seen that the spectral efficiency is degraded significantly for CP-OFDM. In contrast, the proposed system can maintain zero CP within its dispersion tolerance. We also compared the proposed scheme with RGI-OFDM based on frequency domain equalization (FDE). Fig. 3(c) shows the required complex multiplications of RGI-OFDM and the proposed scheme. In the figure, we only consider the complexity of the demultiplexing stage because the complexities of phase and channel estimation etc. are similar. The total complexity of the proposed scheme is $Nx/2 \cdot \log_2(N) + 3Nx/2$ if the memory length of the FIR filters is 2, and is insensitive to dispersion. On the other hand, based on the overlap-and-add principle of RGI-OFDM, the complexity of the RGI-OFDM is obtained as $N/2 \cdot \log_2(N) + (N_{FDE} \cdot \log_2(N_{FDE}) + N_{FDE}) \cdot N / (N_{FDE} - N_{CP})$, where N_{FDE} is the point size of the FDE. This complexity increases as distance increases, and is higher than that of the proposed scheme with $x = 4$ and 8 when the dispersion value is larger than 20,000 and 40,000 ps/nm, respectively. In addition, RGI-OFDM cannot support dispersion values larger than 60,000 ps/nm even with 2048 FDE point size.

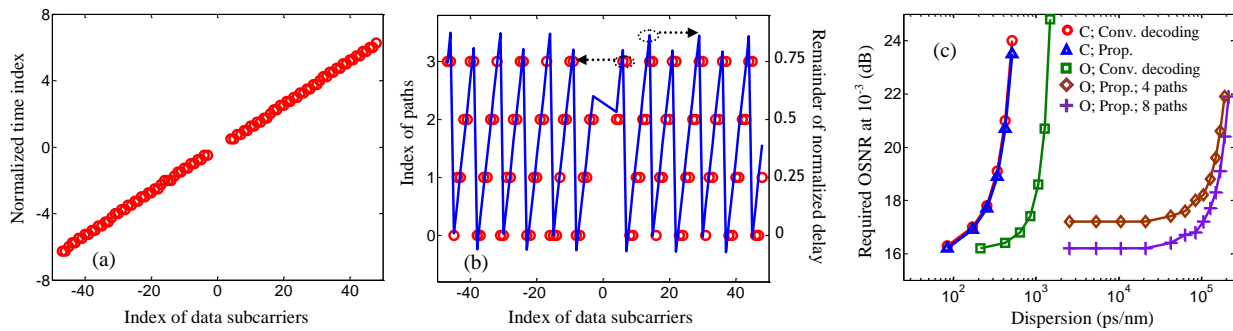


Fig. 2 (a) Normalized time index to decode different subcarriers. (b) The index of paths to decode different subcarriers (circles) and the remainder of normalized delays of subcarriers (solid). The number of subcarriers is 128 (that for data is 90). In (a) and (b), the dispersion is 42,500 ps/nm and x is 4. (c) Required OSNR versus dispersion for conventional CP-OFDM (C) and offset-QAM OFDM (O) when CP is not used.

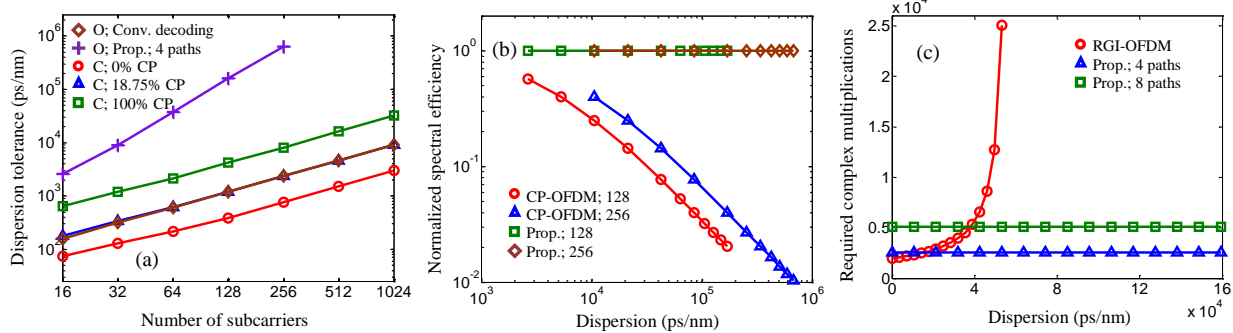


Fig. 3 (a) Dispersion tolerance at an OSNR of 20 dB versus the number of subcarriers for CP-OFDM (C) using different lengths of CP and offset-QPSK OFDM (O) without CP. $x = 4$. (b) Normalized spectral efficiency versus dispersion for 128 and 256 subcarriers. (b) Required complexity of RGI-OFDM and the proposed scheme. The number of subcarriers and the point size of the FDE are 128 and 2048, respectively.

4. Conclusion

We have proposed a novel offset-QAM OFDM scheme that greatly improves the dispersion tolerance by N times without any CP. This scheme exhibits enhanced spectral efficiency, larger dispersion tolerance, and/or reduced complexity compared to CP- and RGI-OFDM. This work was supported by Science Foundation Ireland under grant number 11/SIRG/I2124, EU 7th Framework Program under grant number 318415 (FOX-C), and Hong Kong Research Grant Council GRF14200914.

References

1. J. Zhao et al, "Offset-QAM based coherent WDM for spectral efficiency enhancement," *Opt. Express* **19**, 14617-14631 (2011).
2. J. Zhao, "DFT-based offset-QAM OFDM for optical communication," *Opt. Express* **22**, 1114-1126 (2014).
3. J. Zhao, "Channel estimation in DFT-based offset-QAM OFDM systems," *Opt. Express* **22**, 25651-25662 (2014).
4. J. Zhao et al, "Dispersion tolerance enhancement using an improved offset-QAM OFDM scheme," *Opt. Express* **23**, 17638 (2015).